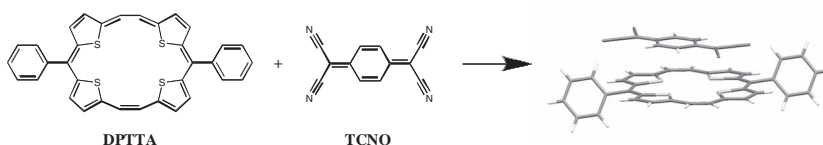


Sulfur-Bridged Annulene-TCNQ Co-Crystal: A Self-Assembled “Molecular Level Heterojunction” with Air Stable Ambipolar Charge Transport Behavior

Jing Zhang, Hua Geng, Tarunpreet Singh Virk, Yan Zhao, Jiahui Tan, Chong-an Di, Wei Xu,* Kamaljit Singh, Wenping Hu, Zhigang Shuai,* Yunqi Liu, and Daoben Zhu*

In recent years, ambipolar organic field-effect transistors (OFETs) have attracted growing research interest because of their potential applications in the organic circuits and organic light-emitting transistors.^[1] Till now, ambipolar transistors have been realized by two major ways: single component transistors based on an ambipolar transport material^[2,3] and two-component transistors with the combination of *p*-type and *n*-type semiconductors.^[4–6] Ambipolar transport materials are particularly desirable concerning the construction of complementary-like circuits, as the fabrication processes could be significantly simplified when two unipolar materials were replaced with an ambipolar material. Despite the huge progresses in organic semiconductors, the ambipolar transport materials are still rare with respect to unipolar materials, and it is still a great challenge in design and synthesis of π -conjugated systems that could fulfill the requirement for achieving both stable *p*-type and *n*-type transport in ambient condition. As an alternative choice, construction of heterostructures with *p*-type and *n*-type semiconductors constitutes an efficient way to realize ambipolar operation. For example, bilayer heterojunction,^[4] bulk heterojunction^[5] and lateral heterostructure^[6] have been successfully demonstrated to fabricate



Scheme 1. Chemical structure of *meso*-diphenyl tetrathia[22]annulene[2,1,2,1] and TCNQ and the molecular structure of the resulted DPTTA-TCNQ complex.

ambipolar transistors. These achievements allow construction of heterojunction with molecular level order possible, namely a cocrystal of existing *p*-type and *n*-type organic semiconductors which offer the advantage similar to that of the one component ambipolar organic semiconductors and avoid the complicated synthesis processes. Here, we present the ambipolar transport behavior of a crystal of neutral donor-acceptor complex formed by *meso*-diphenyl tetrathia[22]annulene[2,1,2,1] (DPTTA) and tetracyanoquinodimethane (TCNQ) in 1:1 ratio (**Scheme 1**). Donor-acceptor π - π interaction is one of the main nonbonding interactions for self-assembly and self-organization of organic molecules, which has been widely studied for the construction of molecular machines, molecular switches and so on.^[7] With charge neutrality in nature, it will be easy to tune the energy level by choosing appropriate molecules to form the complex. Such neutral complex system provides a novel strategy for the construction of ambipolar devices and has great potential for light-emitting transistors.

Tetrathia[22]annulene[2,1,2,1]s are porphyrin like aromatic macrocycles, which display *p*-type transport properties in vacuum deposited thin films.^[8] Among these materials, the *meso*-diphenyl substituted one, DPTTA was a moderate electron donor with a HOMO energy level of -4.88 eV and possesses hole mobility of 0.25 cm² V⁻¹ s⁻¹ in thin films.^[8b] TCNQ is a well studied organic electron acceptor, which possesses high electron mobility up to 1.6 cm² V⁻¹ s⁻¹ in single crystals.^[9] Due to the coplanar structure of DPTTA and TCNQ, a donor-acceptor complex is expected to form when these two molecules are mixed in the same solution. It could be observed from the UV-vis absorption spectrum that no charge transfer occur between DPTTA and TCNQ in the ground state in chlorobenzene with a concentration of 1 mg ml⁻¹ (Figure S1). The single crystal of DPTTA-TCNQ complex suitable for X-ray analysis was obtained by slow evaporation of the aforementioned solution. The crystallographic data were summarized in Table S1. The complex forms a triclinic unit cell and belongs to *P*-1 space group with the unit cell parameters $a = 7.842(1)$ Å, $b = 10.332(1)$ Å,

J. Zhang, Dr. H. Geng, Y. Zhao, J. Tan, Dr. C. Di,
Dr. W. Xu, Prof. W. Hu, Prof. Y. Liu, Prof. D. Zhu
Beijing National Laboratory for Molecular Sciences
Key Laboratory of Organic Solids
Institute of Chemistry
Chinese Academy of Sciences
Beijing 100190, P. R. China
E-mail: wxu@iccas.ac.cn; zhudb@iccas.ac.cn



Prof. Z. Shuai
Chemistry Department
Tsinghua University
Beijing, China
E-mail: zgshuai@tsinghua.edu.cn

T. S. Virk, Prof. K. Singh
Organic Synthesis Laboratory
Department of Applied Chemical Sciences & Technology
Guru Nanak Dev University
Amritsar-143005, India

J. Zhang, Y. Zhao, J. Tan
Graduate University of Chinese Academy of Sciences
Beijing 100049, P. R. China

DOI: 10.1002/adma.201200578

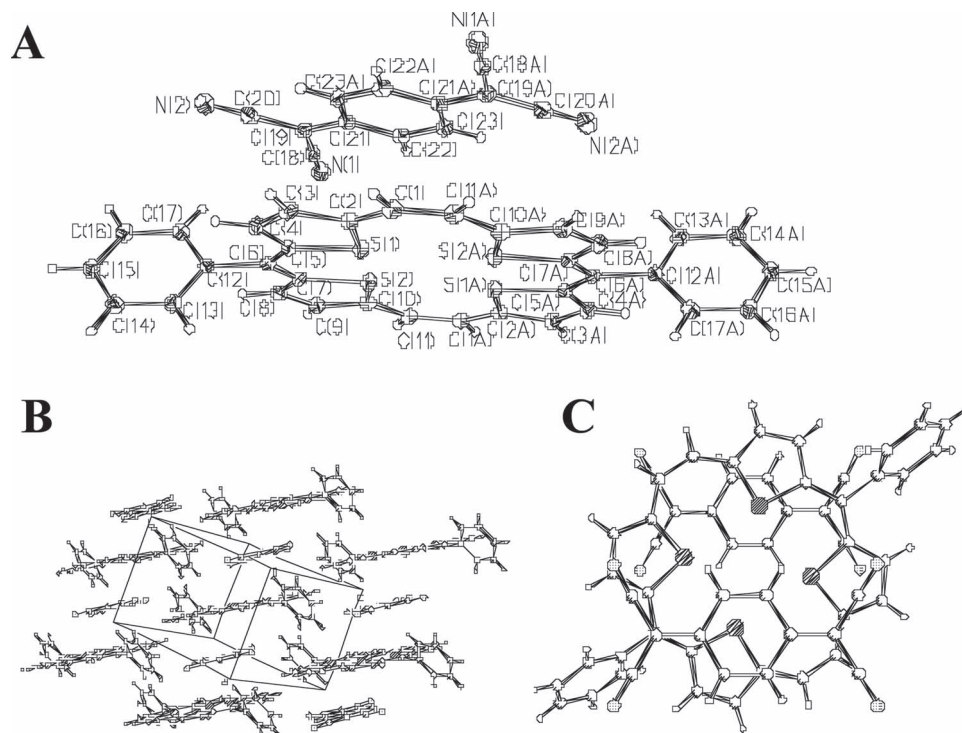


Figure 1. Crystal structure of the DPTTA-TCNQ cocrystal. A) Molecular structure of DPTTA-TCNQ with 50% probability ellipsoids; Crystal packing of DPTTA-TCNQ: B) Alternative stacking pattern and C) Overlap pattern between DPTTA and TCNQ (view perpendicular to the DPTTA plane).

$c = 11.203(1) \text{ \AA}$, $\alpha = 99.911(6)^\circ$, $\beta = 94.616(9)^\circ$, $\gamma = 92.692(8)^\circ$. The molecular structure of DPTTA-TCNQ in crystal is shown in **Figure 1A**. The center tetrathia[22]annulene[2,1,2,1] moiety of DPTTA adopted a nearly coplanar structure with S(1), S(2), S(1A) and S(1B) derived from the mean plane of 0.05, 0.07, -0.05 and -0.07 \AA , respectively. A dihedral angle of $3.46(4)^\circ$ was observed between the molecular plane of DPTTA and TCNQ. The intermolecular distance between DPTTA and TCNQ is around 3.4 \AA , slightly less than that of the typical distance for van der Waals interaction, while a strong non-bonding interaction between N(2) and C(8) (3.158 \AA) could be observed between these two molecules. It has been suggested that the degree of charge transfer in a complex can be estimated by the geometry of TCNQ.^[10] The ratio $c/(b+d)$ related the length of three bonds in TCNQ (indicated in Figure S2) was 0.476 for DPTTA-TCNQ complex, which is the same as the value in neutral TCNQ (0.476). This result indicates that there was no charge transfer between DPTTA and TCNQ. This was further corroborated by the measured CN stretching frequency (2224 cm^{-1}), which is very close to that of the neutral TCNQ (2223 cm^{-1}).^[11]

Similar to that of the complexes of TCNQ with other acene donors such as tetracene, perylene and coronene, DPTTA and TCNQ stack alternatively into a one dimensional column structure along the a -axis, the same molecules in different columns show same tilt angles (Figure 1B). With the relatively small volume, TCNQ molecules were isolated

from each other by the adjacent DPTTA molecules. The face-to-face stacking resulted in complete overlap between TCNQ molecule and half of the DPTTA plane (Figure 1C). Although, there is no continuous separate π -stacking of donor or acceptor molecules in the crystal, the lateral interactions between DPTTA molecules or TCNQ molecules in adjacent columns could be observed, which could serve as the conducting channels for hole and electron, respectively. This issue is discussed in detail in the following section concerning with the intermolecular electronic coupling (or transfer integral).

For transistor device fabrication, a drop-casting method was employed for the preparation of microcrystals of DPTTA-TCNQ complex, which is a simple and easy-going technique to grow high-quality single crystals of organic semiconductors.^[12] As shown in **Figures 2A**, microribbons of single crystal of the

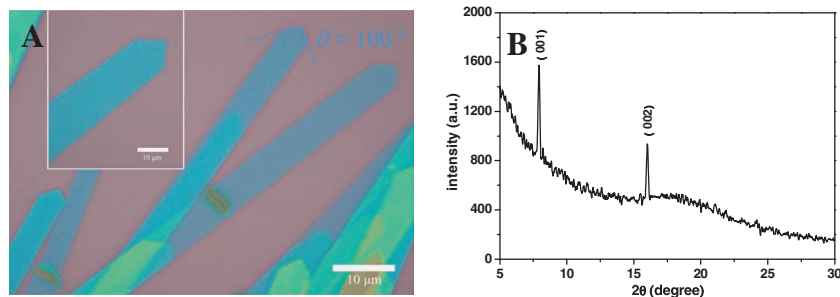


Figure 2. A) Optical images of numbers and individual DPTTA-TCNQ cocrystal microribbons obtained by the drop-casting method. B) Power diffraction pattern of the ribbons. The peaks were indexed with lattice constants of the bulk crystal.

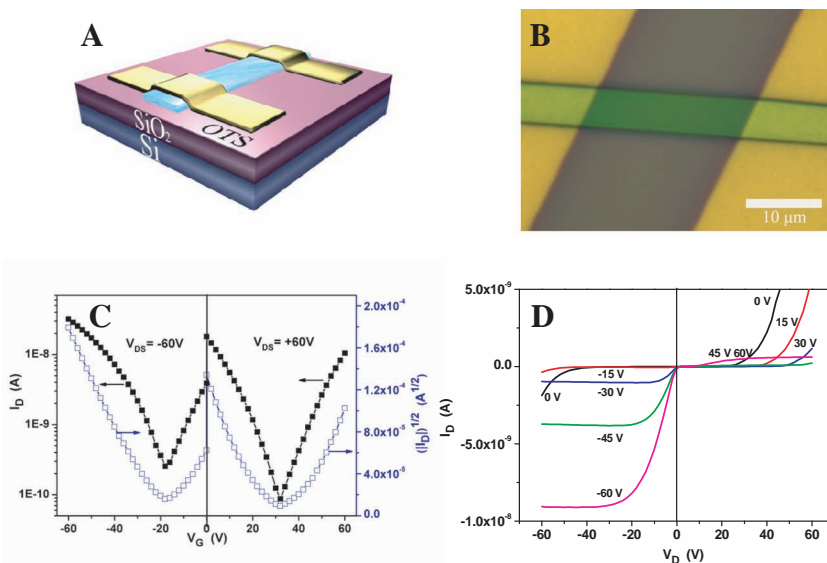


Figure 3. A) Schematic diagram and B) optical image of the device with an individual single crystal. C) Transfer and D) output characteristics (channel length, $L = 43.7 \mu\text{m}$, channel width, $W = 6.0 \mu\text{m}$) of the device.

neutral donor-acceptor complex with a width from several micrometers to tens of micrometers, and a length from tens to hundreds of micrometers was obtained by evaporating of a drop of a mixture of DPTTA and TCNQ in chlorobenzene on OTS/SiO₂/Si substrate (for details, see the Experimental section). The powder X-ray diffraction patterns of the ribbons (Figure 2B) showed an intense peak at (001), (002) in the crystallographic data of DPTTA-TCNQ cocrystal, which was totally different from that of the simulated diffraction patterns of pure DPTTA and TCNQ. This indicates that the structure of the micrometer crystals was identical to that of the bulk crystals of DPTTA-TCNQ complex. And the growth direction of the crystal is determined to be along *a*-axis, the stacking direction (indicated in Figure S3).

Au source/drain electrodes were thermally evaporated on to the microcrystals to construct transistors with the bottom-gate top-contact geometry. Figure 3A and 3B show a schematic representation and an optical microscopy image of one cocrystal transistor with this structure. 20 devices were measured in air and at room temperature and all of them showed typical ambipolar properties. The typical transfer and output characteristics of the heterojunction microribbon device measured are shown in Figure 3C and 3D. From the transfer characteristics, the electron and hole field-effect mobilities (μ) were calculated as $0.03 \text{ cm}^2 \text{ V}^{-1} \text{ s}^{-1}$ (μ_e) and $0.04 \text{ cm}^2 \text{ V}^{-1} \text{ s}^{-1}$ (μ_h), respectively. It should be noted that the devices experienced no obvious degradation in mobility after a period of two months storage in the ambient environment. The performances of the transistors were stable in air, indicating the excellent environmental stability of these ambipolar transistors. CMOS-like inverters have been constructed in a very simple way using two identical transistors built on one single crystal. As shown in the circuit schematic, a common gate (Si) has been used for both the transistors. With negative supply (V_{dd}) and input (V_{in}) voltages, the inverters work with a maximum gain of 10 (Figure S4).

Recently, ambipolar transport behaviors have been observed in single crystals of mixed-stack charge transfer complexes (BEDT-TTF)(F₂TCNQ)^[13] and DBTTF-TCNQ^[14] (BEDT-TTF = bis(ethylenedithio)tetrathiafulvalene, DBTTF = dibenzotetrathiafulvalene). Very high charge carrier mobilities have been predicted theoretically on such charge transfer complex crystals by Zhu et al.^[15] Besides these TTF-like donor based crystals, there are also theoretical predictions on ambipolar behaviors of acene-TCNQ complexes,^[16] but no experimental achievements have yet been reported with acene-TCNQ crystals. For achieving ambipolar transport in single crystal of charge transfer complex, a lot of conditions should be satisfied simultaneously, such as matching of the Fermi energy of electrodes with the energy level of frontier orbitals of the semiconductors; proper contact of the surface of dielectric substrate and the crystal; high quality crystal with sufficient low concentration of trap state and structure defects; crystal structure with electronic band structure favoring to the hole and electron transport. So, it is really a great challenge to achieve ambipolar OFETs based on one single crystal.^[17–19] Here, DPTTA-TCNQ is the first example of neutral donor-acceptor complex crystal which displays typical ambipolar transport behaviors. Comparing to ambipolar transistors based on two different type organic single crystals (such as single-crystalline sub-micrometer-sized ribbons of F₁₆CuPc and CuPc),^[17] organic/inorganic hybrid single-crystals^[18] and even single-crystalline *p-n* junction nanoribbons,^[19] this donor-acceptor cocrystal provides a novel easy processible approach towards ambipolar OFETs and CMOS-like circuits based on micro-scale crystals.

As the first example of co-crystals without charge transfer between the donor and acceptor molecules but displays ambipolar transport properties, DPTTA-TCNQ provides good opportunities for further theoretical investigation on transport properties of such binary component system. Here, we would like to present some preliminary calculation results on this aspect.

Regardless of charge transport mechanism, charge mobility will increase with electronic coupling and decrease with local electron-phonon coupling (reorganization energy). Therefore electronic structure calculations have been performed through B3LYP functional and 6-31G(d) basis sets implemented in Gaussian09,^[20] essentially similar reorganization energy has been found (for electron 256 meV and hole 232 meV).

As can be seen from Figure S5, the valence band (VB) and conduction band (CB) widths are 326 and 327 meV, respectively, with the largest dispersion occurring along the stacking direction and all other directions possessing small contribution to the bandwidths. Nearly mirror symmetry between the CBs and VBs has been found, which suggests that the electronic couplings (transfer integrals) for hole and electron are very similar along the stacking direction. The bottom of VB is dominated by the highest occupied molecular orbitals (HOMO) of donor, and the top of CB by the lowest unoccupied molecular orbitals

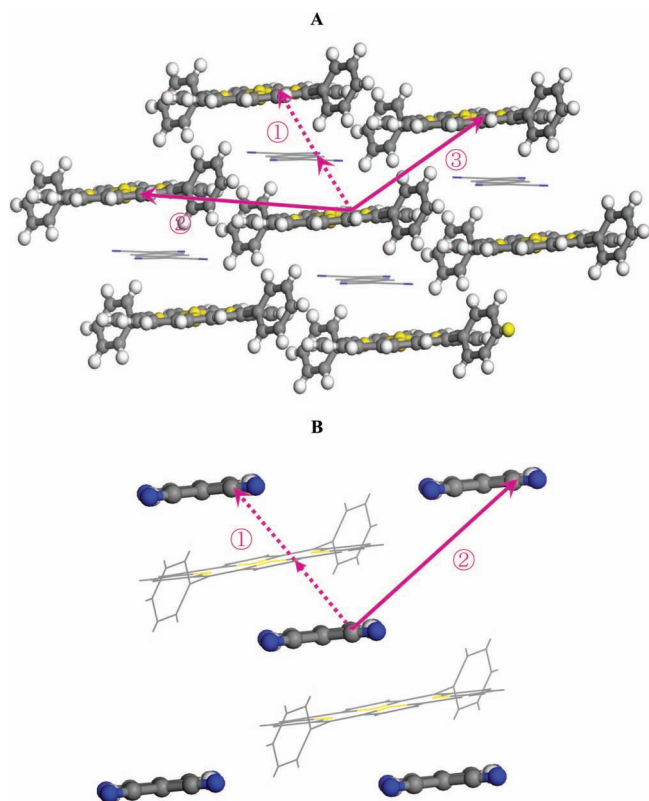


Figure 4. Illustration of the most important charge transport pathways and electronic coupling for hole and electron. (A) Hole: $t_{direct_1}^{hole} = 0$ meV, $t_2 = 8.1$ meV, $t_3 = 7.6$ meV. (B) Electron: $t_{direct_1}^{electron} = 0$ meV, $t_2 = 10.9$ meV.

(LUMO) of the acceptor. Intermolecular bonding (antibonding) interactions induce valence (conduction) dispersion. However it should be noted that acceptor (donor) molecule also contributes to the VB (CB) width via the super-exchange effect in the electronic coupling.

Molecular stacking and direct D-D (A-A) electronic coupling through space is illustrated in **Figure 4**. The direct electronic coupling along π stacking is zero, other directions also display relatively small direct coupling. In case of the alternatively mixed donor-acceptor stack, super-exchange effects must be considered.^[21] We built D-A-D and A-D-A clusters to evaluate the acceptor (donor) bridge contribution to the electronic couplings between donor (acceptor) molecules and effective electronic couplings can be obtained through molecular orbital splitting method.^[15] The detailed calculation approach to compute the effective transfer integrals along the stacking directions is illustrated in **Figure 5**. The obtained transfer integrals are similar for hole and electron (62, 63 meV), in good agreement with the band-structure. This rationalizes that the hole and electron mobilities are observed close each other along the a -axis in the crystal.

In contrast to bulk heterojunction, this mixed donor-acceptor stacking complex offers construction of a heterostructure at molecular level order, which could be named as “molecular level heterojunction”. High performance and stability could be expected when device fabricated based on such crystalline materials. More importantly, this “molecular level heterojunction” was self-assembled from a solution-grown mixed-stack donor-acceptor complex based on DPTTA and TCNQ. Devices based on such high ordered structure exhibited ambipolar behavior with stable balance hole mobility of $0.04 \text{ cm}^2 \text{ V}^{-1} \text{ s}^{-1}$ and electron mobility of $0.03 \text{ cm}^2 \text{ V}^{-1} \text{ s}^{-1}$ in ambient atmosphere. It provides a novel easy-to-process approach to realize ambipolar transport and has great potential for low-cost devices and CMOS-like circuits.

Experimental Section

Materials: Meso-diphenyl tetrathia[22]annulene[2,1,2,1] was synthesized as reported.^[8b] TCNQ were purchased from Aldrich Chemical Company and purified by gradient sublimation once before use.

Growth of the Micro-crystals and Device Fabrication: The SiO_2/Si substrate was heavily doped n-type Si wafer with a 500 nm thick SiO_2 layer and a capacitance of $7.5 \text{ nF}\cdot\text{cm}^{-2}$. Bare substrates were successively cleaned with pure water, piranha solution ($\text{H}_2\text{SO}_4:\text{H}_2\text{O}_2 = 2:1$), pure water and pure isopropanol. Treatment of Si/SiO_2 wafer with OTS used in the present study was carried out by vapor deposition method. The clean wafers were dried under vacuum at 90°C for 0.5 h in order to eliminate the influence of the moisture. After cooling to room temperature, a little drop of OTS was placed on the wafers. Subsequently, this system was heated to 120°C and maintained for 2 h under vacuum. Micrometer-sized single crystals of the donor-acceptor complex were conducted by using the drop-casting method. A chlorobenzene solution containing DPTTA and TCNQ ($1\text{--}2 \text{ mg mL}^{-1}$, molar ratio 1:1) was poured over the substrates and the solvent evaporated at room temperature. Drain and source Au electrodes (40 nm thick) were deposited on the crystal by thermal evaporation with a copper grid as the shadow mask.

Measurements: UV-vis spectra were taken on a Hitachi U-3010 spectrometer. SEM images were obtained with a Hitachi S-4800 SEM (Japan). X-ray diffraction (XRD) was measured on D/max2500 with CuK α source ($\kappa = 1.541 \text{ \AA}$). I - V characteristics of the OFETs were recorded with a Keithley 4200 SCS and a Micromanipulator 6150 probe station

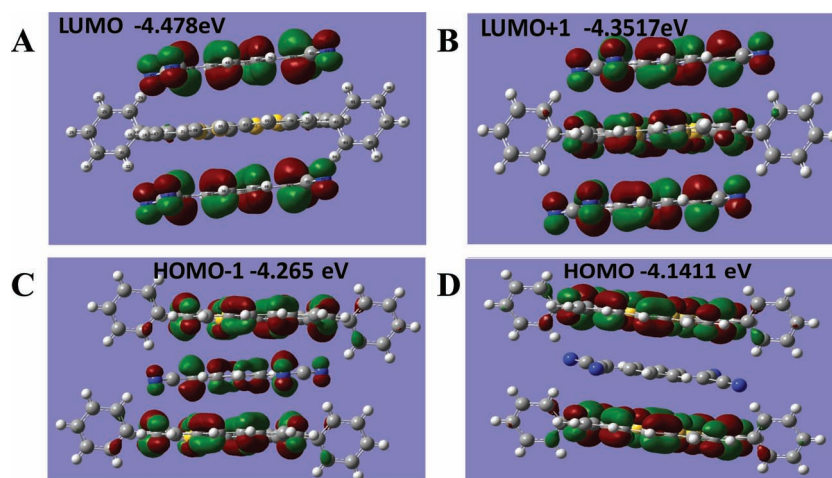


Figure 5. Transfer integrals along stacking direction based on energy-splitting method. $t_{eff_1} = (E_{L+1} - E_L)/2 = 63$ meV, $t_{eff_2} = (E_{H-1} - E_H)/2 = 62$ meV.

in a clean and shielded box at room temperature. X-ray crystallographic data were collected with a Bruker Smart-1000-CCD diffractometer, using graphite-monochromated Mo K α radiation ($\lambda = 0.71073 \text{ \AA}$). The data were collected at 113 K and the structure was resolved by the direct method and refined by the full-matrix least-squares method on F^2 . The computations were performed with the SHELXL-97 program.^[22] The final refinement was anisotropic for all non-H atoms.

Quantum simulations: Based on crystal structure data, first-principles band structure calculations are performed by the projector-augmented wave method with the LDA functional as implemented in VASP.^[23] A plane-wave cutoff energy of 450 eV and $4 \times 4 \times 4$ Monkhorst–Pack k-mesh are adopted in calculation.

Supporting Information

Supporting Information is available from the Wiley Online Library or from the author.

Acknowledgements

The authors acknowledge the financial support from National Natural Science Foundation of China (20952001, 21021091), the State Key Basic Research Program (2011CB808401, 2011CB932304) and Chinese Academy of Sciences. KS thanks DST, New Delhi for financial assistance. Supporting Information is available online from Wiley InterScience or from the author.

Received: February 10, 2012
Published online: April 13, 2012

- [1] a) J. Zaumseil, H. Sirringhaus, *Chem. Rev.* **2007**, *107*, 1296; b) E. J. Meijer, D. M. Deleeuw, S. Setayesh, E. V. Veenendaal, B. H. Huisman, P. W. M. Blom, J. C. Hummelen, U. Scherf, T. M. Klapwijk, *Nat. Mater.* **2003**, *2*, 678; c) F. Dinelli, R. Capelli, M. A. Loi, M. Murgia, M. Muccini, A. Facchetti, T. J. Marks, *Adv. Mater.* **2006**, *18*, 1416.
- [2] a) C. Liu, Z. Liu, H. T. Lemke, H. N. Tsao, R. C. G. Naber, Y. Li, K. Banger, K. Müllen, M. M. Nielsen, H. Sirringhaus, *Chem. Mater.* **2010**, *22*, 2120; b) M. L. Tang, A. D. Reichardt, N. Miyaki, R. M. Stoltenberg, Z. Bao, *J. Am. Chem. Soc.* **2008**, *130*, 6064; c) A. R. Mohebbi, J. Yuen, J. Fan, C. Munoz, M. f. Wang, R. S. Shirazi, J. Seifert, F. Wudl, *Adv. Mater.* **2011**, *23*, 4644; d) C. Rost, S. Karg, W. Riess, M. A. Loi, M. Murgia, M. Muccini, *Synth. Met.* **2004**, *146*, 237.
- [3] a) F. S. Kim, X. Guo, M. D. Watson, S. A. Jenekhe, *Adv. Mater.* **2010**, *22*, 478; b) Y.-Y. Liu, C.-L. Song, W.-J. Zeng, K.-G. Zhou, Z.-F. Shi, C.-B. Ma, F. Yang, H.-L. Zhang, X. Gong, *J. Am. Chem. Soc.* **2010**, *132*, 16349.
- [4] a) R. Ye, M. Baba, K. Jpn. Mori, *J. Appl. Phys.* **2005**, *44*, 581; b) J. Wang, H. B. Wang, X. J. Yan, H. C. Huang, D. Jin, J. W. Shi, Y. H. Tang, D. H. Yan, *Adv. Funct. Mater.* **2006**, *16*, 824.
- [5] a) C. Rost, S. Karg, W. Riess, M. A. Loi, M. Murgia, M. Muccini, *Appl. Phys. Lett.* **2004**, *85*, 1613; b) E. J. Meijer, D. M. de Leeuw, S. Setayesh, E. van Veenendaal, B. H. Huisman, P. W. M. Blom, J. C. Hummelen, U. Scherf, T. M. Klapwijk, *Nat. Mater.* **2003**, *2*, 678; c) M. Shkunov, R. Simmes, M. Heeney, S. Tierney, I. McCulloch, *Adv. Mater.* **2005**, *17*, 2608.
- [6] a) J.-F. Chang, M. C. Gwinner, M. Caironi, T. Sakanoue, H. Sirringhaus, *Adv. Funct. Mater.* **2010**, *20*, 2825; b) Z. Wei, W. Xu, W. Hu, D. Zhu, *J. Mater. Chem.* **2008**, *18*, 2420.
- [7] a) D. B. Amabilino, J. F. Stoddart, *Chem. Rev.* **1995**, *95*, 2725; b) G. Koshkaryan, L. M. Klivansky, D. Cao, M. Snauko, S. J. Teat, J. O. Struppe, Y. Liu, *J. Am. Chem. Soc.* **2009**, *131*, 2078; c) L. Y. Park, D. G. Hamilton, E. A. McGehee, K. A. McMenimen, *J. Am. Chem. Soc.* **2003**, *125*, 10586.
- [8] a) T. Zhao, Z. Wei, Y. Song, W. Xu, W. Hu, D. Zhu, *J. Mater. Chem.* **2007**, *17*, 4377. b) K. Singh, A. Sharma, J. Zhang, W. Xu, D. Zhu, *Chem. Commun.* **2011**, 47, 905.
- [9] E. Menard, V. Podzorov, S.-H. Hur, A. Gaur, M. E. Gershenson, J. A. Rogers, *Adv. Mater.* **2004**, *16*, 2097.
- [10] a) T. J. Kistenmacher, T. J. Emge, A. N. Bloch, D. O. Cowan, *Acta Crystallogr.* **1982**, *B38*, 1193; b) X. Chi, C. Besnard, V. K. Thorsmølle, V. Y. Butko, A. J. Taylor, T. Siegrist, A. P. Ramirez, *Chem. Mater.* **2004**, *16*, 5751.
- [11] J. S. Chappell, A. N. Bloch, W. E. Bryden, M. Maxfield, T. O. Poehler, D. O. Cowan, *J. Am. Chem. Soc.* **1981**, *103*, 2442.
- [12] a) M. Mas-Torrent, M. Durkut, P. Hadley, X. Ribas, C. Rovira, *J. Am. Chem. Soc.* **2003**, *126*, 984; b) L. Jiang, Y. Fu, H. Li, W. Hu, *J. Am. Chem. Soc.* **2008**, *130*, 3937.
- [13] T. Hasegawa, K. Mattenberger, J. Takeya, B. Batlogg, *Phys. Rev. B*, **2004**, *69*, 245115.
- [14] Y. Takahashi, T. Hasegawa, Y. Abe, Y. Tokura, G. Saito, *Appl. Phys. Lett.* **2006**, *88*, 073504.
- [15] L. Zhu, Y. Yi, Y. Li, E.-G. Kim, V. Coropceanu, J. Bredas, *J. Am. Chem. Soc.* **2012**, *134*, 2340.
- [16] I. Shokaryev, A. J. C. Buurma, O. D. Jurchescu, M. A. Uijtewaal, G. A. de Wijs, T. T. M. Palstra, R. A. de Groot, *J. Phys. Chem. A*, **2008**, *112*, 2497.
- [17] Q. Tang, Y. Tong, H. Li, Z. Ji, L. Li, W. Hu, Y. Liu, D. Zhu, *Adv. Mater.* **2008**, *20*, 1511.
- [18] Y. Zhang, Q. Tang, H. Li, W. Hu, *Appl. Phys. Lett.* **2009**, *94*, 203304.
- [19] Y. Zhang, H. Dong, Q. Tang, S. Ferdous, F. Liu, S. C. B. Mannsfeld, W. Hu, A. L. Briseno, *J. Am. Chem. Soc.* **2010**, *132*, 11580.
- [20] GAUSSIAN09, Revision A.02, M. J. Frisch, G. W. Trucks, H. B. Schlegel, G. E. Scuseria, M. A. Robb, J. R. Cheeseman, G. Scalmani, V. Barone, B. Mennucci, G. A. Petersson, H. Nakatsuji, M. Caricato, X. Li, H. P. Hratchian, A. F. Izmaylov, J. Bloino, G. Zheng, J. L. Sonnenberg, M. Hada, M. Ehara, K. Toyota, R. Fukuda, J. Hasegawa, M. Ishida, T. Nakajima, Y. Honda, O. Kitao, H. Nakai, T. Vreven, J. A. Montgomery Jr., J. E. Peralta, F. Ogliaro, M. Bearpark, J. J. Heyd, E. Brothers, K. N. Kudin, V. N. Staroverov, R. Kobayashi, J. Normand, K. Raghavachari, A. Rendell, J. C. Burant, S. S. Iyengar, J. Tomasi, M. Cossi, N. Rega, J. M. Millam, M. Klene, J. E. Knox, J. B. Cross, V. Bakken, C. Adamo, J. Jaramillo, R. Gomperts, R. E. Stratmann, O. Yazyev, A. J. Austin, R. Cammi, C. Pomelli, J. W. Ochterski, R. L. Martin, K. Morokuma, V. G. Zakrzewski, G. A. Voth, P. Salvador, J. J. Dannenberg, S. Dapprich, A. D. Daniels, Ö. Farkas, J. B. Foresman, J. V. Ortiz, J. Cioslowski, D. J. Fox, *Gaussian, Inc.*, Wallingford CT, **2009**.
- [21] a) S. Larsson, *J. Am. Chem. Soc.* **1981**, *103*, 4034; b) S. Yin, M. G. Dahlbom, P. J. Canfield, N. S. Hush, R. Kobayashi, J. R. Reimers, *J. Phys. Chem. B*, **2007**, *111*, 9923.
- [22] G. M. Sheldrick, (1997)SHELXL97, Program for the Refinement of Crystal Structure, University of Göttingen, Germany.
- [23] G. Kresse, J. Furthmüller, *Phys. Rev. B*, **1996**, *54*, 11169.